Time-zero detector based on microchannel plates and a friable dielectric emitter

S.M. Lukyanov, M. Lewitowicz, Yu.E. Penionzhkevich, G.G. Chubarian, D. Bazin, D. Guillemaud-Mueller, A.C. Mueller, M.G. Saint-Laurent

GANIL

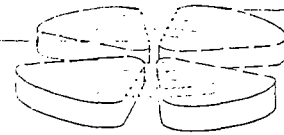

TIME-ZERO DETECTOR BASED ON MICROCHANNEL PLATES AND A FRIABLE DIELECTRIC EMITTER

by

S.M. Lukyanov[1]), M. Lewitowicz[2]), Yu.E. Penionzhkevich[1]), C.G. Chubarian[3]), D. Bazin[4]), D. Guillemaud-Mueller[4]), A.C. Mueller[4]), M.G. Saint-Laurent[4]).

[1]) JINR, Dubna, USSR
[2]) Polish Atomic Agency, Warsaw, Poland
[3]) Yerevan Institute of Physics, Yerevan, USSR
[4]) GANIL, Caen, France

GANIL P.86.21

S.M. Lukyanov[1], M. Lewitowicz[2], Yu.E. Penionzhkevich[1],
C.G. Chubarian[3], D. Bazin[4], D. Guillemaud-Mueller[4], A.C. Mueller[4],
M.G. Saint-Laurent[4].

TIME-ZERO DETECTOR BASED ON MICROCHANNEL PLATES AND A FRIABLE DIELECTRIC EMITTER

1) JINR, Dubna, USSR
2) Polish Atomic Agency, Warsaw, Poland
3) Yerevan Institute of Physics, Yerevan, USSR
4) GANIL, Caen, France

I - INTRODUCTION

In the recent years the time-of-flight technique was widely used to determine the mass of heavy-ion reaction products. One of the reasons for that is the possibility of using the transmission detectors based on microchannel plates (MCP) for measuring the time-of-flight of passing particles[1-4]. The main advantages of such detectors are a high time resolution (intrinsic time resolution of about 70-100 ps), the reliability and simple design.

A MCP is used in time-zero detectors as a fast multiplier of secondary electrons emitted by charged particles passing through a foil and then isochronously collected with a magnetic[1] or electrostatic[2] systems on the MCP's mounted in a chevron configuration.

The typical multiplication factor for a configuration with two MCP is 10^6-10^7.

For the measurements of fission fragments or fission-like products (with an energy ~ 2 MeV/n emitters) from thin (10-30 $\mu g/cm^2$) organic or carbon foils give an efficiency of about 100 %. For high-energy reaction products, however, these emitters are inadaquate because of the very low (<1) secondary electron emission coefficient[6]. For example, for ^4He with an energy of 7.5 MeV/n the efficiency of detection was only a few percent for a trinitrocellulose emitter[6].

One of the most effective and simplest way to increase the detection efficiency is, in our view, to use emitters with control of secondary electron emission (CSEE) by means of friable dielectrics[7,8].

The CSSE is the process of electron emission from the layer of a friable dielectric in the strong electric field produced between two electrodes placed on both sides of the layer.

The friable dielectric layers are produced by evaporation in a vacuum of CsI, KCl or LiF salts onto a support which is used, at the same time as one of the electrodes. The evaporation is provided in an inert gas at a pressure of several torrs, whereas layers of magnesium oxide (MgO) are obtained by deflagration of polycrystalline magnesium in thin air and by depositing its oxide onto a support. Depending on the evaporation conditions (the deflagration temperature, the distance between magnesium and collecting supports, air pressure, deposition time, etc) it is possible to obtain layers with a thickness from 30 $\mu g/cm^2$ to several mg/cm^2 with a relative density ρ/ρ_0 ranging from 0.3 to serveral percent (ρ_0 being the density of a MgO monocrystal). As a result of that evaporation process, a friable dielectric emitter with the channel structure presented in fig. 1, is produced. The investigations of CSEE show that for friable dielectrics the coefficient of secondary electron emission in an electric field of $E > 3 \times 10^4$ V/cm is more than 10^2 times greater than that for normal solids[7]. This fact can be explained as follows : the emission of electrons occurs from the entire volume of a friable dielectric and then their number is multiplied in the intrinsic channels in the strong electric field. In such an interpretation the CSEE process is very similar to the electron multiplication in a MCP[9].

II - DESCRIPTION OF THE TIME-ZERO DETECTOR

The principle of operation and design features of our detector are analogous to those presented in ref.[2]. Fig. 2 shows a schematic view of the detector. The detector consists of five parts : a CSEE emitter with a MgO layer, an acceleration harp, an electrostatic mirror, two MCP's in a chevron configuration and a flat anode. A MgO dielectric has been chosen because of its high nonhygroscopic properties (in contrast to other

dielectrics such as CsI, KCl and LiF) and, at the same time, of its very good electron emission characteristics. A layer of MgO was evaporated onto a nickel grid with a thin (~ 10 $\mu g/cm^2$) trinitrocellulose foil as a backing. In order to obtain a high multiplication coefficient at an acceleration of emitted electrons to an energy of about 1 KeV, an electric field of 5×10^4 V/cm is applied between the grid-support of MgO and the accelerating harp. After bending in the electrostatic mirror through 90° the electrons were collected on the MCP's where their number is multiplied by 10^6-10^7 times. Output pulses are obtained from a flat anode placed under the MCP's. The main characteristics of our detector are presented un table 1.

III - EXPERIMENTAL TESTS WITH A HEAVY-ION BEAM

1) Experimental set-up

A test of the detector has been performed with a heavy-ion beam from the GANIL accelerator. $^{16}O^{8+}$ ions with an energy of 50 MeV/n bombarded a gold target (thickness ~ 100 mg/cm^2). The reaction products were selected by the LISE magnetic spectrometer/10/. The time-zero detector was mounted after the second dipole magnet of the spectrometer (Fig. 3). At about 6 m downstream a 1 mm thick ΔE semiconductor detector was placed at the achromatic refocusing point of the spectrometer. In order to sustain a not too high counting rate for the ΔE detector the spectrometer was set to a magnetic rigidity corresponding to the transmission of (helium-like) $^{16}O^{6+}$. The spectrometer was limited to a momentum acceptance of $\Delta p/p = 0.2$ %. The output pulse from the time-zero detector was directely fed to a 7174 Enertec constant fraction discriminator (CFD). The time signal derived from the ΔE detector by means of a fast preamplifier and another constant fraction discriminator served as a START input for a 566 ORTEC time-to-amplitude converter (TAC) which was stopped by the delayed timing signal of the

time-zero detector.

The start and stop input had been reversed in order to not untimely trigger the TAC on background pulses from the MCPS. The output pulses from the TAC were analysed by a SILENA (Cato) multichannel analyser.

2) Results

The efficiency of the detector depends of course strongly on the discrimination threshold. For the actual oxygen beam, representing the "worst case" of a light ion of high energy (i.e. small energy loss), an efficiency of 70 % was found for a discriminator threshold of 70 mV, decreasing to 50 % for a setting of 150 mV.

The result of the time resolution measurement is shown in Fig. 4a), where a FWHM of 360 ps is obtained. This value is consistent with a convolution of several contributions which have to be taken into account :

i) the time-of-flight of the oxygen particles over the 6 m distance amounts to 65 ns which, since $\Delta p/p$ = 0.2 % lead to a width of ~130 ps of the beam itself.

ii) the intrinsic width of the time-zero detector (~ 100 ps)

iii) the "walk" of the constant fraction discriminator. This contribution is relatively large since the input pulses cover a wide span. From the operating manual of the CFD a value of 270 ps is found for an input between several volts and the threshold setting.

iv) the width induced by the ΔE detector timing chain (~ 150 ps)

Fig. 4b) shows for comparaison, the resolution which is obtained by stopping the TAC by the radio-frequency pulse of GANIL accelerator in lieu of the signal from the time-zero detector. A FWHM of 680 ps is observed.

This value is still relatively good and associated to the very satisfactory operation of the new ECR ion source for gaseous materials. For metallic ions however, produced by the PIG source, values of up to 2 ns have been found, accompagnied by occasionnal phase shifts of several ns. Here the use of a time-zero detector of the proposed type will apport a substancial improvement.

The test of the detector will be persued with heavier beams in order to obtain a complete picture of its potential and performance.

REFERENCES

1. A.M.Zebelman et al. Nucl.Instr.and Meth., v.141, (1977), p.439.
2. F.Busch et al. Nucl.Instr. and Meth., v.171, (1980), p.71.
3. A.Oed et al. Nucl.Instr. and Meth., v.179 (1981), p.265.
4. R.Kotte, G.Ortlepp, F.Stary, S.M.Lukyanov, Workshop on heavy ions experiments, Varna, 1984, JINR D7-84-736, Dubna 1984.
5. V.D.Dmitriev et al. Sov. Journal Devices and Methods of Experiments, N 2, 1981,p.7.
6. R.L.Kavalov et al. Sov. Journal Devices and Methods of Experiments, N 3, 1982, p.46.
7. N.P.Lorikan et al. Nucl.Instr. and Methods, v.122, 1974, p.377.
8. N.N.Trofimchuk et al. Sov. Journal of Experimental and Theoretical Physics, v.69, N 8, 1975, p.639.
9. A.N.Arvanov et al. Soviet Journal of Radio-engineering and electronics, v.27, N 1, 1982, p.163.
10. R.Anne, C.Signarbieux, GANIL RA/NU 278, 1982.

TABLE 1

I - Secondary electron emitter

. grid-support : Ni wires, 92 % transparency, layer of trinitrocellulose with thickness ~ 10 $\mu g/cm^2$

. friable dielectric : MgO with relative density $\rho/\rho_o < 1\%$ ($\rho_o = 3.65\ g/cm^3$), thickness > 100 $\mu g/cm$. accelerating harp : Be-bronze wires with Ø 90 μm, step between wires, 1mm.

. electric field, $E > 10^4$ V/cm

II - Electrostatic mirror

. two parallel harps (same as accelerating harp), distance between them : 7.5 mm.

III - Electron multiplier

. 2 MCP in a chevron configuration, Ø 56 mm each, distances MCP-MCP and MCP-anode 1 mm each,

. anode : Ø 60 mm flat,

. multiplication factor 10^6-10^7 at high voltage, 2.2 - 2.5 kV.

Figure Captions

Fig. 1. Electron microscope photograph of the friable dielectric layer (MgO) evaporated onto a grid-support.

Fig. 2. Schematic view of the time-zero detector.

Fig. 3. Experimental set-up.

Fig. 4. Time-of-flight spectra for $^{16}O^{6+}$ ions measured in the systems :

a) time-zero detector-semiconductor ΔE detector,

b) time-zero detector - CSS2 accelerator radio frequency

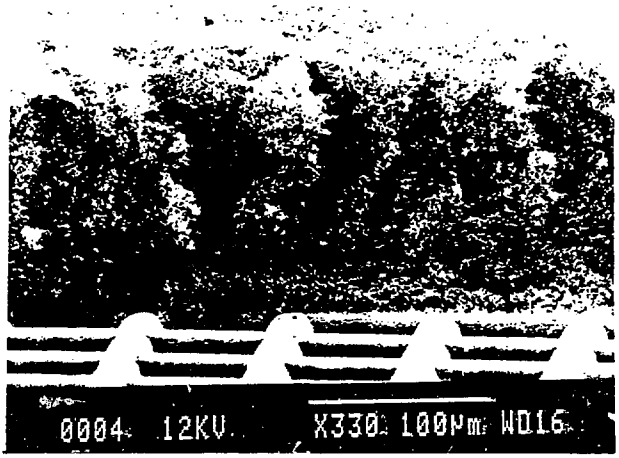

Fig. 1

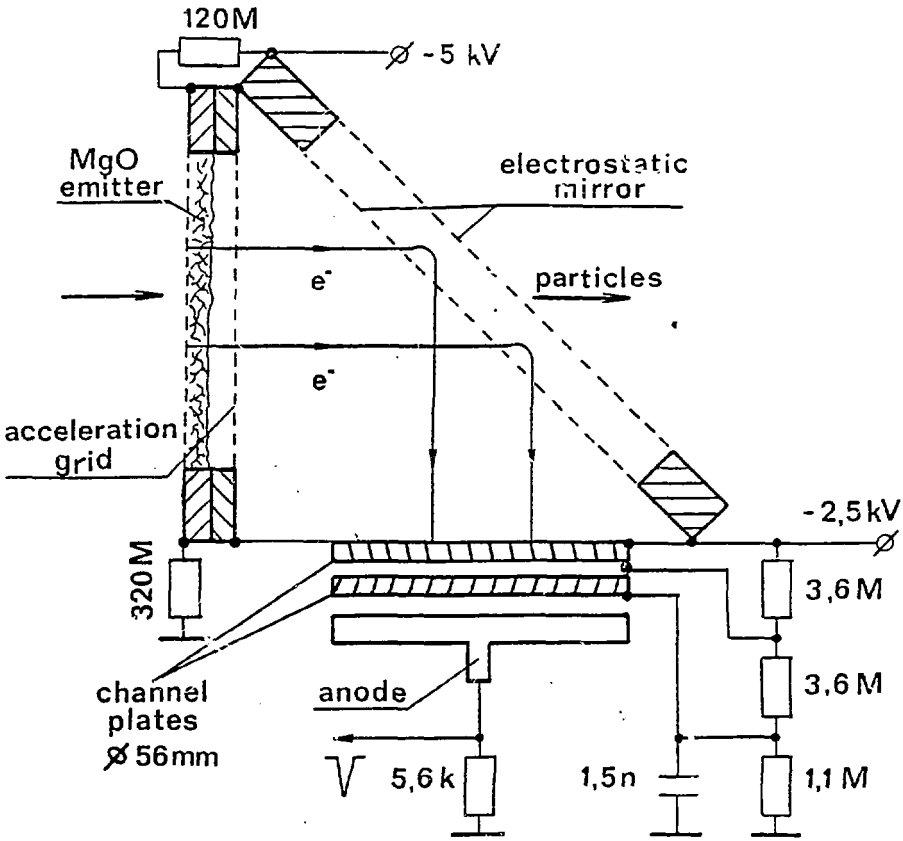
120M
-5 kV
MgO
emitter
electrostatic
mirror
e⁻
particles
e⁻
acceleration
grid
-2,5 kV
320M
3,6 M
3,6 M
channel
plates
Ø 56mm
anode
5,6 k
1,5 n
1,1 M

Fig. 2

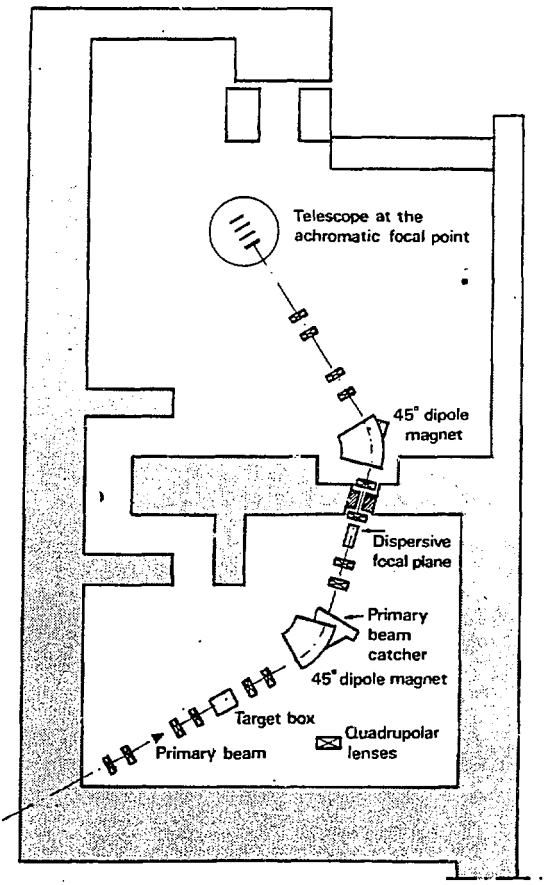
Telescope at the
achromatic focal point
45° dipole
magnet
Dispersive
focal plane
Primary
beam
catcher
45° dipole magnet
Target box
Primary beam
Quadrupolar
lenses

Fig. 3

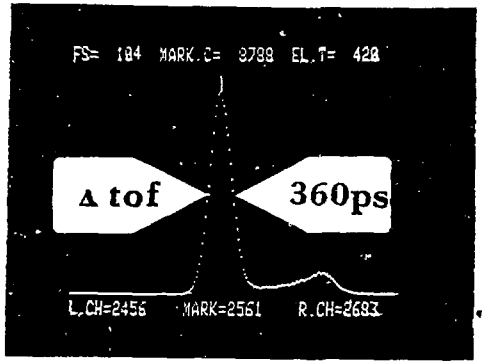
FS= 184 MARK.C= 8788 EL.T= 420
Δ tof
360ps
L.CH=2456 MARK=2561 R.CH=2683

a)

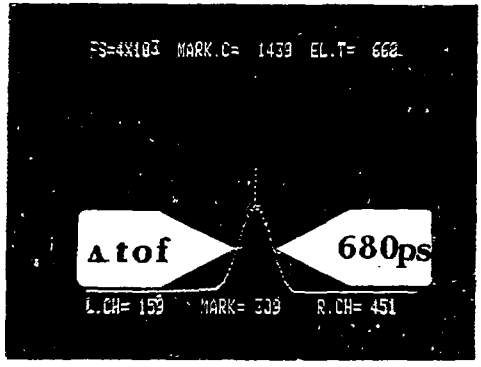
FS=4X183 MARK.C= 1439 EL.T= 660
Δ tof
680ps
L.CH= 159 MARK= 339 R.CH= 451

b)

Fig. 4